Estimation of Cost-based Channel Occupancy in Cognitive Radio Using Sequential Monte Carlo Methods

by

Joseph Zapp

A Thesis Presented in Partial Fulfillment
of the Requirement for the Degree
Master of Science

Approved April 2014 by the
Graduate Supervisory Committee:

Antonia Papandreou-Suppappola, Chair
Narayan Kovvali
Martin Reisslein

ARIZONA STATE UNIVERSITY

May 2014

ABSTRACT

Dynamic channel selection in cognitive radio consists of two main phases. The first phase is spectrum sensing, during which the channels that are occupied by the primary users are detected. The second phase is channel selection, during which the state of the channel to be used by the secondary user is estimated. The existing cognitive radio channel selection literature assumes perfect spectrum sensing. However, this assumption becomes problematic as the noise in the channels increases, resulting in high probability of false alarm and high probability of missed detection. This thesis proposes a solution to this problem by incorporating the estimated state of channel occupancy into a selection cost function.

The problem of optimal single-channel selection in cognitive radio is considered. A unique approach to the channel selection problem is proposed which consists of first using a particle filter to estimate the state of channel occupancy and then using the estimated state with a cost function to select a single channel for transmission. The selection cost function provides a means of assessing the various combinations of unoccupied channels in terms of desirability. By minimizing the expected selection cost function over all possible channel occupancy combinations, the optimal hypothesis which identifies the optimal single channel is obtained.

Several variations of the proposed cost-based channel selection approach are discussed and simulated in a variety of environments, ranging from low to high number of primary user channels, low to high levels of signal-to-noise ratios, and low to high levels of primary user traffic.

Dedicated to my uncle Robert (RIP), who continues to inspire me, and to my lovely wife Mary, who keeps me motivated and helped me to persevere through my graduate studies.

$\sim$

To my precious daughter Alaina, who I could always count on to crawl up to the computer and provide much needed distractions throughout the long hours spent working on this thesis.

$\sim$

To mom and dad.

$\sim$

To my high school teachers, Mr. Peter Gayner and Mr. David Weissing, both of whom instilled in me a love of and appreciation for mathematics and engineering.

ACKNOWLEDGEMENTS

I would like to thank all of my committee members: Professor Antonia Papandreou-Suppappola, Dr. Narayan Kovvali, and Professor Martin Reisslein.

Special thanks to Professor Antonia Papandreou-Suppappola for recommending I write a thesis, for suggesting cognitive radio as the topic, and for advising me throughout the process. I have found this work to be highly rewarding, and the topic to be very interesting. Had it not been for her, this work would not have been started.

Also, special thanks to Dr. Narayan Kovvali for his many hours of assistance in helping to formulate my ideas into something anyone other than myself would understand. And of course for providing his own invaluable input. Without his help, this work probably would not have been finished.

TABLE OF CONTENTS

Page

CHAPTER Page

LIST OF TABLES

LIST OF FIGURES

Chapter 1

INTRODUCTION

1.1 Work Motivation

Cognitive radio is a disruptive radio communications and networking technology [1], which enables radios to perform dynamic channel selection (DCS). DCS is a cyclic process consisting of three phases. During the first phase, the radio senses spectrum consisting of multiple primary user channels in order to detect which channels are occupied. During the second phase, the radio selects a single channel from the list of unoccupied channels. The radio transmits over the selected channel during the third phase. The concept of a DCS-capable radio is of great interest to the wireless communications industry because it provides a solution to the problem of spectrum scarcity by making more efficient use of existing radio spectrum [2]. Gaps, or spectrum holes, can be found in the spectrum at various times and frequencies when licensed primary users are not transmitting. The DCS-capable radio provides an unlicensed secondary user the opportunity to transmit over a licensed primary user channel, essentially filling in the gaps.

The main problem that must be addressed in DCS deals with primary user channel occupancy. Specifically, at each time step, the occupancy of each primary user channel must be determined. This problem, which is solved by means of various spectrum sensing techniques, has received a great deal of attention in the research community [2, 3, 4, 5, 6, 7]. Another important problem in DCS is channel selection [8, 9, 10]. Once the primary user channel occupancy is determined, the secondary user must select a single channel out of all the detected unoccupied channels to use for transmission.

Channel selection has not received as much attention as spectrum sensing in the research community. However the choice of an adequate channel selection technique is important in order to minimize the number of channels the secondary user has to switch from. This is because switching channels can be quite costly as it can cause unnecessary delays in transmission and an increase in the packet loss ratio [11].

Some of the existing channel selection methods include works discussed in [11-14], where perfect spectrum sensing is assumed under high signal-to-noise ratio (SNR) conditions. In [11], learning automata techniques are used to converge on the optimal channel selection decision in order to avoid channel switches. Here, the optimal channel is considered to be the channel with the lowest overall probability of primary user occupancy. In [12], the channel selection problem in a multi-channel network, with multiple secondary users and multiple primary users, is addressed. This paper focuses on optimizing the channel selection operation by maximizing the total channel utilization across all secondary users. This is performed by minimizing the probability of contention for the same available channel by multiple secondary users. In [13], the question of optimal bandwidth allocation for secondary users is addressed. Multiple channels can be selected by a single secondary user for transmission, allowing for higher throughput. This is, however, at the cost of an increase in the number of channel switches due to an increase in likelihood that one of the primary users will return to reclaim a channel. This paper also includes a study on the tradeoff between the number of channels selected and the overall throughput. In [14], the problem of channel selection is explored from a standpoint of maximizing secondary user throughput. Different primary user channels are assumed to offer different levels of bandwidth. As a result, if the primary user returns to the channel that the secondary user selected, then the secondary user must decide whether to move to a different channel or wait for the channel to become unoccupied again.

The aforementioned methods of channel selection do not take into consideration the cost of a secondary user dynamically selecting a channel based on prior knowledge on the previously selected channel. Also, although models on channel transition have been previously considered [14, 15, 16], the models have not been used to dynamically estimate the true state of the primary user channels. To our knowledge, a cost-based channel selection approach which makes use of particle filter to estimate the state of channel occupancy has not been proposed.

1.2 Proposed Work

The primary objective of this work is to optimize the channel selection phase of DCS. We achieve this objective by first using the particle filter (PF) sequential Monte Carlo method [17] to estimate the true state of primary user channel occupancy, and then by using the estimated state in a cost-based selection approach. In particular, we minimize the expected cost of a selection cost function over all possible channel selection scenarios in order to determine the optimal channel selection. Our intent is to first obtain a more accurate estimate of the state of channel occupancy and then to use that estimate with a selection cost function to optimize channel selection by not only minimizing channel switches, but also by minimizing primary user interference and secondary user missed opportunities.

In our work, we consider a single secondary user operating within a network consisting of multiple primary users. Each primary user transmits over a contiguous band of frequencies which we collectively refer to as a channel. Primary user channels are assumed to be completely independent. The secondary user is capable of sensing a bandwidth consisting of multiple primary user channels simultaneously at each time step according to a given probability of false alarm and probability of detection. A channel is considered to be available to the secondary user for transmission at time

step k if the primary user is not transmitting at time step k. Multiple channels can be available at each time step, but only a single channel can be selected by the secondary user for transmission.

We assume that the transmission patterns of the primary user in each channel follow a statistical channel occupancy model that is fixed with respect to time, and is known to the secondary user. We also assume that the spectrum sensing measurements made by the secondary user follow a statistical measurement model that is fixed with respect to time. But unlike the channel occupancy model, the measurement model is identical across all channels.

As the focus of our work is on the channel selection phase of DCS, we assume that spectrum sensing was already performed using one of the existing techniques, and that the results of the spectrum sensing operation, along with the statistical measurement model parameters (i.e., probability of false alarm (P_{FA}) and probability of detection (P_{D})) are available as inputs to the channel selection phase. The output of the channel selection phase is a single channel that is used by the secondary user for transmission at time step k. We assume that any coordination between the secondary user source-destination pair, choice of transmission power, modulation type, etc., is handled during the transmission phase of DCS. The transmission phase is outside the scope of our work.

1.3 Organization of Thesis

The thesis is organized as follows. In Chapter 2, we provide a brief overview of cognitive radio technology, and we discuss radio frequency spectrum and its current availability. In Chapter 3, we discuss DCS at a high level and provide an overview of each of the individual steps of the DCS cycle. In Chapter 4, we discuss our channel occupancy state and measurement models, and show how the particle filter is used

to estimate the state of primary user channel occupancy. In Chapter 5, we present our cost selection function and show how it is used to select the optimal channel. In Chapter 6, we discuss our simulation parameters and results. Finally, in Chapter 7, we provide some concluding remarks and suggestions for future work.

Chapter 2

COGNITIVE RADIO AND SPECTRUM ALLOCATION

This chapter introduces cognitive radio as an assortment of technologies capable of solving the spectrum availability problems that the wireless communications industry is now facing.

An overview of cognitive radio is provided in Section 2.1. The current state of spectrum availability is discussed in Section 2.2. The fixed spectrum allocation policies currently in use are discussed in Section 2.3.

2.1 Cognitive Radio Overview

Cognitive radio is a term used to describe a new class of self-aware radios [18]. It can be thought of an intelligent wireless communication system that adapts to its environment to achieve highly reliable communications and efficient radio spectrum utilization [19]. The term is used interchangeably to describe both the radio itself, and the technologies within the radio that make it cognitive. No single technology makes a radio cognitive. Rather, an assortment of technologies are combined to form a cognitive radio in order to benefit the radio user or the radio network. The technologies, when viewed individually may not be new or breakthrough. What is new is the way in which the technologies are integrated to create a smarter radio.

The enabling technology of cognitive radio is software defined radio. This is a technology that allows software to control certain radio parameters such as carrier frequency, signal bandwidth, modulation, and network access [20]. With the technology in place to dynamically configure these parameters, software defined radio was

then combined with other technologies such as artificial intelligence, geo-location, and spectrum sensing in order to provide new and significant benefits to radio users and radio networks [18]. One of the most significant of these benefits is the more efficient use of radio spectrum.

2.2 Spectrum Availability

Although the electromagnetic spectrum is effectively infinite, only a portion of it has the necessary propagation characteristics that make it suitable for wireless radio communications. This portion of the electromagnetic spectrum, as shown in Figure 2.1, is commonly referred to as the radio spectrum. Because radio communications channels must reside within this portion of the electromagnetic spectrum, the radio spectrum can be thought of as a finite, physical resource. As is the case with most of the worlds physical resources, over time, use of the radio spectrum has dramatically increased. Demand for spectrum, driven by high-bandwidth cellular and WiFi applications, is on the rise. This has resulted in spectrum scarcity or unavailability for new wireless communications services.

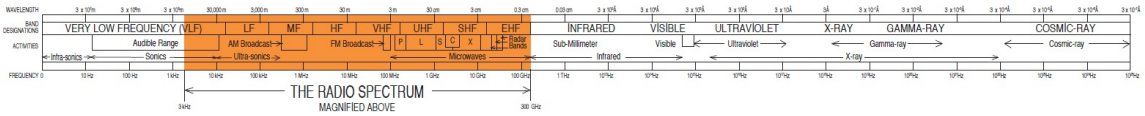

Figure 2.1: The radio spectrum. Figure taken from [21].

Figure 2.2 provides a portion of the United States frequency allocation table where it is clearly demonstrated that nearly one hundred percent of the radio spectrum has already been allocated. In fact, the only portion that has not been allocated is a small portion of low-frequency spectrum that is unusable for high-speed, high-bandwidth applications.

Several advances in wireless communications technology such as ultra-wideband,

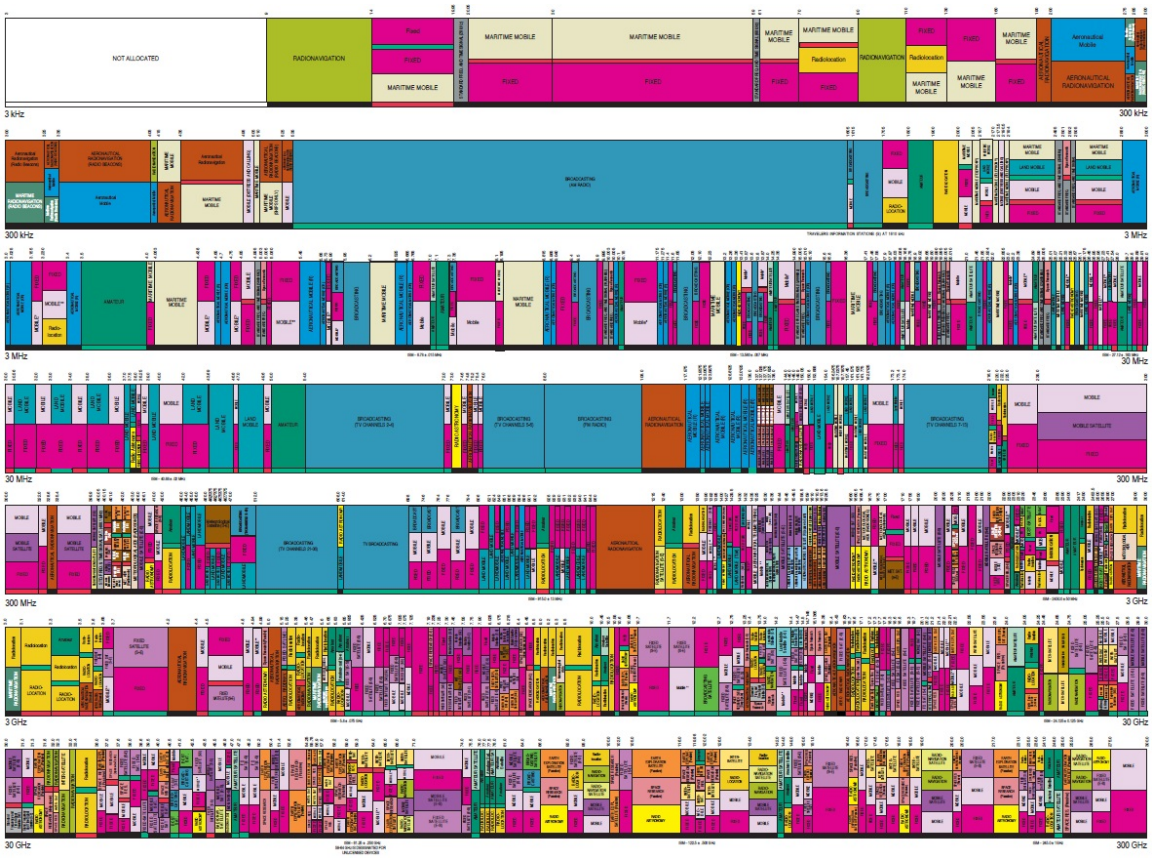

Figure 2.2: United States frequency allocations. Figure taken from [21].

spread-spectrum, and orthogonal frequency-division multiplexing have been implemented to allow for more efficient use of the radio spectrum. In addition to this, research has been done to expand wireless communications to use spectrum outside of the 3 kHz to 300 GHz radio spectrum block. Visible light communication makes use of visible light that ranges in frequency from 400 THz to 800 THz. This form of wireless communication has been shown to transmit data at rates of up to 500 MBit/s over a distance of 5 meters [22]. Visible light communication certainly shows potential for high data-rate communications over short distances, but the propagation characteristics of visible light spectrum greatly limit its usefulness as a wireless communications medium.

2.3 Spectrum Allocation

The root of the spectrum availability problem is that the underlying spectrum allocation policies are inherently inefficient. The easiest way to visualize the inefficiency of radio spectrum allocation policies is to consider the analogy of a very large multi-lane highway. If the lanes of the highway were to be allocated and regulated in a manner similar to that of radio spectrum channels, each lane would be owned by a single entity (a shipping company, for example), and that entity would be guaranteed sole use of the lane. When a company is busy shipping products, there will be many vehicles in its lane, but at other times the lane will be completely empty.

This is precisely what is happening with communications channels in the radio spectrum. At peak times in busy cities, a few communications channels are highly utilized by the entities that own them, but overall, spectrum usage is low. In 2004 and 2005, the Shared Spectrum Company carried out a series of spectrum measurements in several different rural and urban areas in an attempt to quantify how efficiently spectrum was being utilized in the range of 30 MHz to 3 GHz [23]. Measurements were taken over a period of 3 days, and the findings are summarized in Figure 2.3.

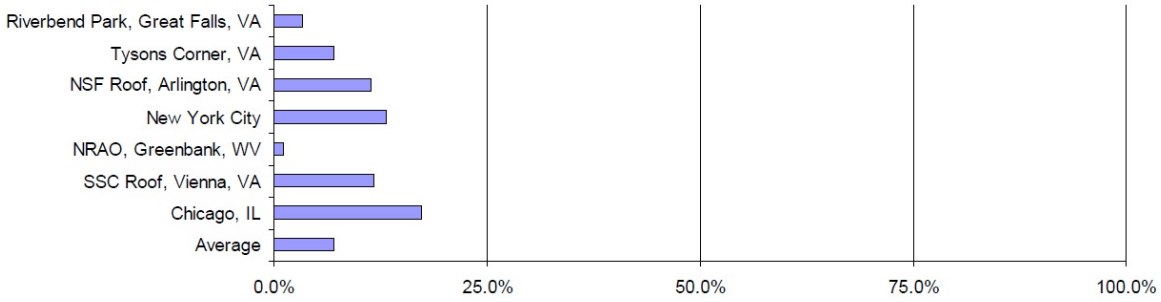

Figure 2.3: Overall spectrum occupancy in different locations. Figure taken from [23].

According to the measurements, Chicago was found to have the highest overall spectrum occupancy at 17.4%, while Greenbank had the lowest at 1%. The average occupancy across the 7 locations was less than 10%. A breakdown of spectrum

occupancy within common spectrum bands, averaged across the 7 locations, is shown in Figure 2.4.

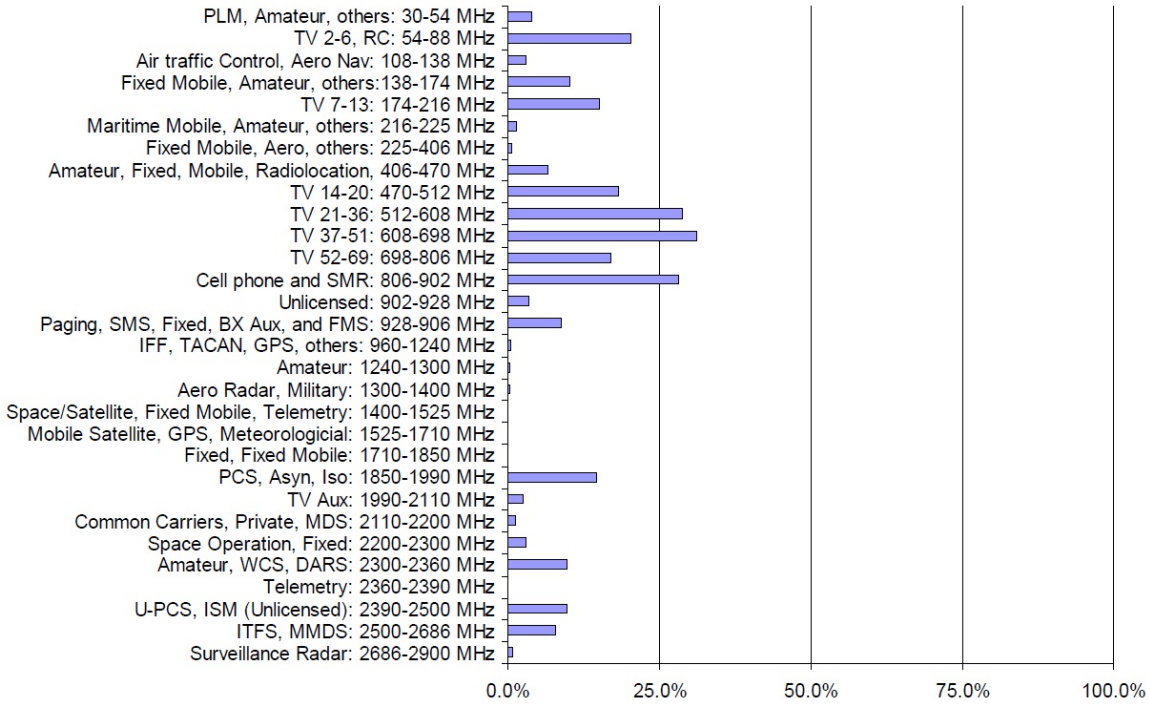

Figure 2.4: Breakdown of spectrum occupancy within common spectrum bands. Figure taken from [23].

We can easily see from Figure 2.3 and Figure 2.4 that spectrum, taken as a whole, across all channels, locations, and times, is underutilized. Using the highway analogy, we know that in reality, highway lanes are not owned by a single entity, but rather shared among all motorists who wish to access the highway. These "smart" motorists are capable of switching lanes as needed to fill in the gaps and utilize each lane to its full potential. This is, in essence, what is meant to be accomplished by a new spectrum allocation paradigm, referred to as dynamic spectrum allocation. According to this paradigm, a channel owned by a primary user may be used opportunistically by a secondary user when the primary user is not using the channel. The benefits of using cognitive radio technology to implement this paradigm were first discussed in [24]. In our work, we refer to the functional implementation of the dynamic spectrum

allocation paradigm in a cognitive radio as dynamic channel selection (DCS).

Chapter 3

DYNAMIC CHANNEL SELECTION OVERVIEW

Dynamic channel selection, also known as dynamic spectrum access or opportunistic spectrum access, is a cyclic process with three distinct phases, as shown in Figure 3.1. The first phase is spectrum sensing. This is the phase in which the secondary user scans its environment in an effort to detect unoccupied channels. The second phase is channel selection. This is the phase in which the secondary user makes a decision to select a single unoccupied channel for transmission. The third phase is transmission. During transmission, the secondary user transmits over the channel selected during the channel selection phase. Although the focus of our work is on the channel selection phase of dynamic channel selection, we briefly discuss the spectrum sensing and transmission phases in order to place our discussion of channel selection within the context of the overall dynamic channel selection cycle.

Spectrum sensing is discussed in Section 3.1. Channel selection is discussed in Section 3.2. Transmission is discussed in Section 3.3.

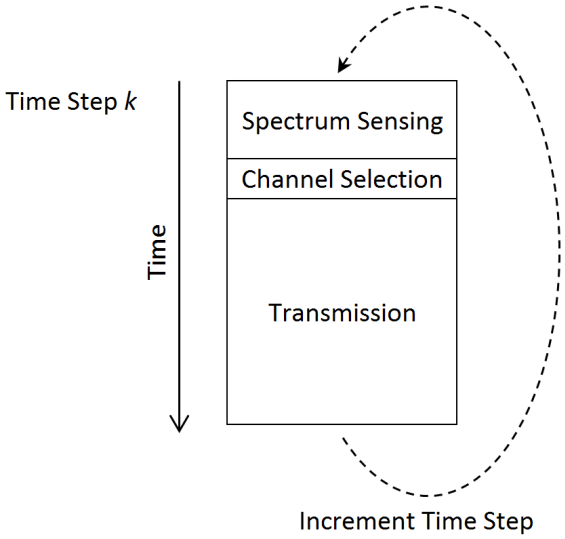

Figure 3.1: Dynamic channel selection cycle.

3.1 Spectrum Sensing

Spectrum sensing is defined in [25] as "the action of a radio measuring signal features". The radio (the unlicensed secondary user) is a cognitive radio capable of dynamic channel selection. Spectrum sensing consists of first using an antenna to passively scan the environment for some length of time, and then processing the sensed signal to derive a decision test statistic. The detection test statistic is then used to decide whether or not the licensed primary user is currently transmitting over the channel [26]. If the primary user is not occupying the channel, then a spectrum hole exists, and the channel can be utilized by the secondary user for transmission over a pre-determined duration of time. After the transmission by the secondary user, the spectrum sensing operation is repeated. The spectrum sensing operation is performed periodically across multiple channels simultaneously.

Spectrum sensing can be represented in the time-frequency plane, as depicted in Figure 3.2. The total spectrum detected by the secondary user has some fixed bandwidth which is sub-divided into N channels. The bandwidth of each individual

channel is known by the secondary user *a-priori*. The sensing time is the amount of time that the secondary user senses the spectrum before moving on to the decision making process on the occupancy of each of the N channels.

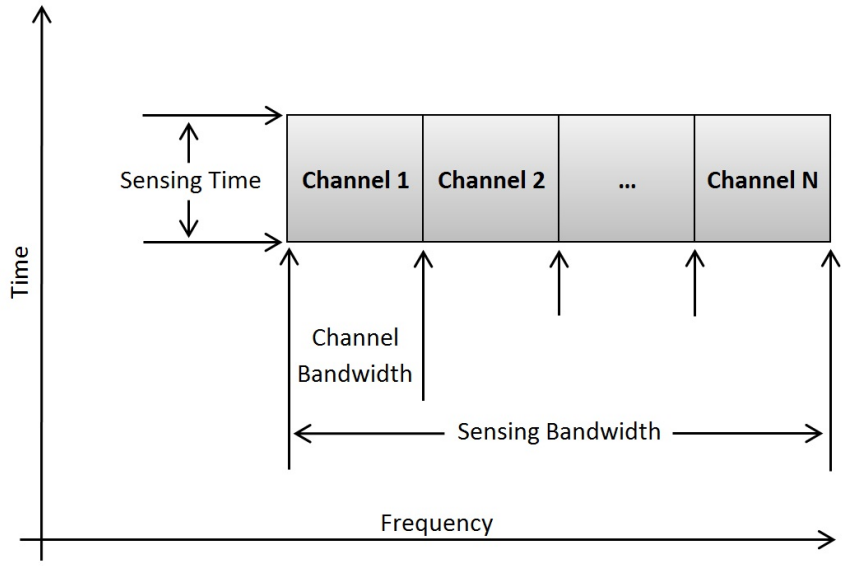

Figure 3.2: Representation of spectrum channel sensing in the the time-frequency plane.

The spectrum sensing decision making process is generally approached as a statistical problem in which two hypotheses are defined. Hypothesis H_0 is used to describe the case in which the primary user signal is not present within a channel (i.e., the channel is unoccupied and a spectrum hole exists). Hypothesis H_1 is used to describe the case in which the primary user signal is present within a channel (i.e., the channel is occupied).

There are two possible types of error, depending on which hypothesis is chosen. The first type of error is false alarm (or false positive); this error occurs when hypothesis H_1 is chosen when H_0 is true. The probability of false alarm (P_{FA}) is an important metric from the standpoint of the secondary user because it represents missed opportunities, and the secondary user can only function properly if it is able

to find sufficient opportunities to transmit. The second type of error is missed detection (or false negative). A missed detection occurs when hypothesis H_0 is chosen when H_1 is true. The probability of missed detection (P_{MD}) is an important metric from the standpoint of the primary user because if the secondary user determines an occupied channel to be unoccupied, and then starts to transmit over the channel, the primary user could suffer some level of interference.

The values of P_{FA} and P_{MD} depend on both the level of signal-to-noise ratio (SNR), and the spectrum sensing technique that is used. Spectrum sensing techniques can be classified as either coherent or non-coherent [5]. Coherent techniques, such as cyclostationary detection and matched filter detection, require *a priori* information about the primary user signal. Non-coherent techniques, such as energy detection, do not require *a priori* information. A survey of a number of different coherent and non-coherent spectrum sensing techniques is provided in [7]. The performance of various spectrum sensing techniques is compared in [4] and [3]. A survey of energy detection spectrum sensing techniques is provided in [5].

Regardless of the technique used, the output of the spectrum sensing operation at time step k is the $(N \times 1)$ vector, $\mathbf{y}_k = [y_{k,1} \dots y_{k,N}]^T$ where T denotes the vector transpose. The vector $\mathbf{y}_k$ provides the measured state of the channel occupancy of the N channels that the cognitive radio is sensing. Each of the N vector elements, $y_{k,i}$, $i = 1, \dots, N$, takes on a value of 1 or 0 depending on whether the ith channel is sensed to be occupied by the primary user at time index k.

$$y_{k,i} = \begin{cases} 0, & i\text{th channel not occupied at time step } k \\ 1, & i\text{th channel occupied at time step } k \end{cases} \tag{3.1}$$

The total number of possible channel states is thus 2^N.

3.2 Channel Selection

The objective of channel selection is to choose the optimal single channel for transmission at time step k. A high-level block diagram depicting this approach is shown in Figure 3.3.

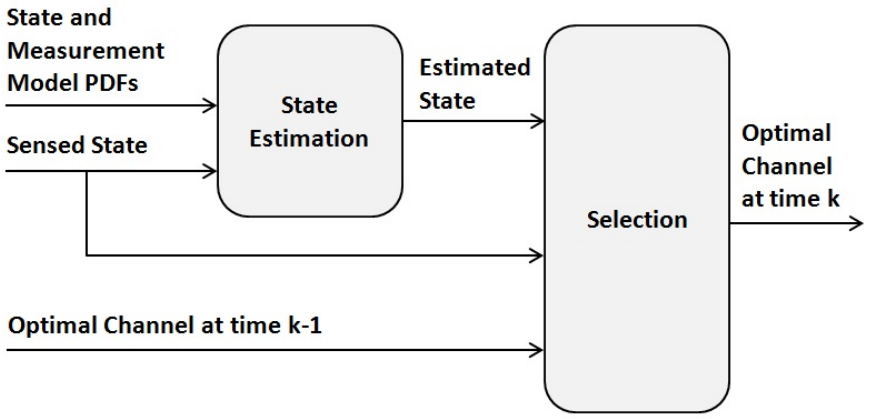

Figure 3.3: Channel selection block diagram.

Each possible channel selection decision that can be made corresponds to one of the N channels that is currently being sensed. In addition, a null decision can also be made if none of the channels is deemed suitable for transmission. If the null decision is selected, then the cognitive radio will not transmit during time step k and must wait until time step $k+1$ for another chance to transmit. The total number of possible decisions at time step k is thus N+1, and they are represented by the set of hypotheses $\{H_k^{(0)}, H_k^{(1)}, \ldots, H_k^{(N)}\}$ where $H_k^{(0)}$ represents the null decision, and $H_k^{(\mathrm{ch})}, \mathrm{ch} = 1, \ldots, N$ represents the decision in which channel ch is selected. The optimal decision denoted by, $\widehat{H}_k^{(\mathrm{ch})}$, provides the channel that minimizes the expected cost over all possible decisions. The optimal decision thus represents the channel that is then used for transmission at time step k.

3.3 Transmission

During the transmission phase, the selected channel is used to transmit voice or data at time step k for some length of time. It is assumed that the selection of transmission parameters in the network, media access control, and physical layers is performed during this phase. We also assume that the selection of these parameters is performed independently from the channel selection optimization process. A few examples of these adjustable transmission parameters are transmitter power, modulation type, symbol rate, encryption, and packet size. In [27], these parameters are described as *writable parameters*, and they can be optimized based on the values of a set of *observable parameters*. A few examples of observable parameters are bit error rate, path-loss, data rate, and packet delay. In [28], in which these writable and observable parameters are referred to as knobs and meters respectively, the optimization of the knobs based on the readings from the meters, is explored as a multi-objective decision-making problem. Note that a further discussion of the transmission phase if beyond the scope of this thesis.

Chapter 4

CHANNEL OCCUPANCY STATE ESTIMATION

Existing cognitive radio channel selection methods often assume that measurements from the spectrum sensing phase provide perfect detection of the unoccupied channels. However, due to variations in signal-to-noise ratio environmental conditions, non-zero probability of false alarm and probability of missed detection need to be taken into consideration when estimating the channel state occupancy. In this chapter, we propose to improve the accuracy of channel occupancy state estimation by formulating and solving the problem as a dynamic state space estimation, where the measurement directly depends on the probability of detection and the probability of false alarm.

In Section 4.1, we formulate the channel occupancy using a dynamic state model; we provide the measurement model that provides information on the channel occupancy state in Section 4.2. In Section 4.3, we discuss the particle filter sequential Monte Carlo method that can be used to provide an estimate of the probability density function of the state given the measurement.

4.1 Channel Occupancy State Model

We consider a cognitive radio application after the spectrum sensing decision making process phase. It was determined that we have N independent and stochastically identical channels that can be modeled using the Gilbert-Elliot channel model [29]. At any given time, the state of a channel can be considered to be occupied or unoccupied by the primary user. We are interested in estimating when the channel is

unoccupied by the primary user in order to provide secondary users with opportunistic spectrum access. As demonstrated in [14-16], a two-state discrete-time Markov chain is a fit model for the channel transitions between occupied and unoccupied states. Denoting the state of the ith channel at time step k as $x_{k,i}$, we demonstrate the two channel states and the channel transition probabilities in Figure 4.1. Specifically, when $x_{k,i} = 0$, the state of the channel is unoccupied and when $x_{k,i} = 1$, the state of the channel is occupied. There are four transition probabilities involved for the ith channel, transitioning from a state at time step $k-1$ to either the same or new state at time step k. For example, from Figure 4.1, $\Pr(x_{k,i} = 1|x_{k-1,i} = 0)$ is the probability that the ith channel transitions from being unoccupied at time step $k-1$ to being occupied at time step k.

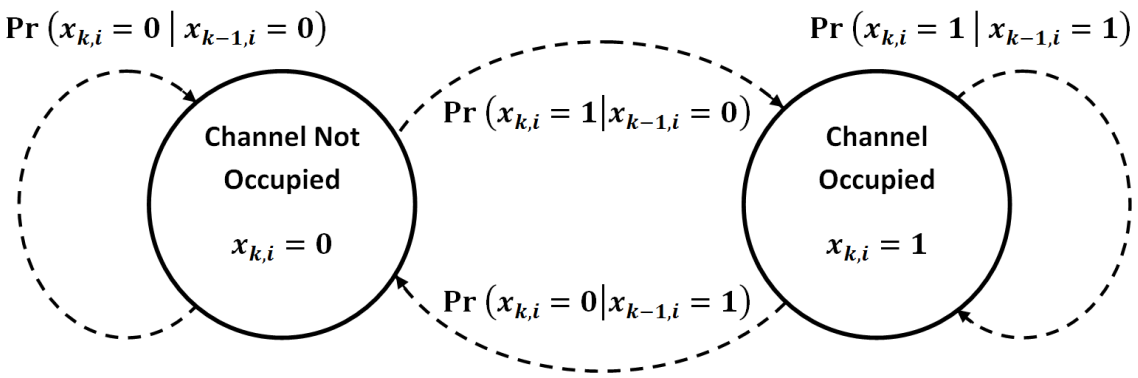

Figure 4.1: Channel occupancy modeled as a two-state discrete-time Markov chain.

The discrete probability density function that defines the state of the ith channel at time step $k = 0$ is given as follows:

$$\mathrm{p}(x_{0,i}) = \Pr(x_{0,i} = 0)\delta[x_{0,i} - 0] + \Pr(x_{0,i} = 1)\delta[x_{0,i} - 1] \tag{4.1}$$

where $\delta[x-1]$ is the Kronecker delta function, defined to be 1 when $x = 1$ and zero otherwise. In (4.1), $\Pr(x_{0,i} = 0)$ is the probability that the state of the ith channel is not occupied at time step $k = 0$ and $\Pr(x_{0,i} = 1)$ is the probability that the state of

the ith channel is occupied at time step $k = 0$.

A formulation of the probability density function describing the channel state model is given by

$$\begin{aligned} \mathrm{p}(x_{k,i}|x_{k-1,i} = 0) =& \Pr(x_{k,i} = 0|x_{k-1,i} = 0)\delta[x_{k,i} - 0] + \\ & \Pr(x_{k,i} = 1|x_{k-1,i} = 0)\delta[x_{k,i} - 1] \end{aligned} \tag{4.2}$$

This is a discrete probability density function that defines the state of the ith channel at time step k, given that the state of the ith channel is not occupied at time step $k-1$. In (4.2), $\Pr(x_{k,i} = 0|x_{k-1,i} = 0)$ is the probability that the state of the ith channel is not occupied at time step k, given that the state of the ith channel is not occupied at time step $k-1$, and $\Pr(x_{k,i} = 1|x_{k-1,i} = 0)$ is the probability that the state of the ith channel is occupied at time step k, given that the state of the ith channel is not occupied at time step $k-1$.

Similarly, the discrete probability density function that defines the state of the ith channel at time step k, given that the state of the ith channel was occupied at time step $k-1$ is given as follows:

$$\begin{aligned} \mathrm{p}(x_{k,i}|x_{k-1,i} = 1) =& \Pr(x_{k,i} = 0|x_{k-1,i} = 0)\delta[x_{k,i} - 0] + \\ & \Pr(x_{k,i} = 1|x_{k-1,i} = 0)\delta[x_{k,i} - 1] \end{aligned} \tag{4.3}$$

where $\Pr(x_{k,i} = 0|x_{k-1,i} = 1)$ is the probability that the state of the ith channel is not occupied at time step k, given that the state of the ith channel is occupied at time step $k-1$, and $\Pr(x_{k,i} = 1|x_{k-1,i} = 1)$ is the probability that the state of the ith channel is occupied at time step k, given that the state of the ith channel is occupied at time step $k-1$.

4.2 Measurement Model

The measurement corresponds to the information $y_{k,i}$ provided at the spectrum sensing phase on the state of the ith channel at time step k; if $y_{k,i} = 0$, then the

measurement provides the information that the channel is not occupied and if $y_{k,i} = 1$, then the information states that the channel is occupied. The measurement model is provided by two discrete probability density functions.

The discrete probability density function that defines the sensed state of the ith channel at time step k, given that the state of the ith channel is not occupied at time step k is given by

$$\begin{aligned} \mathrm{p}(y_{k,i}|x_{k,i} = 0) =& \Pr(y_{k,i} = 0|x_{k,i} = 0)\delta[y_{k,i} - 0] + \\ & \Pr(y_{k,i} = 1|x_{k,i} = 0)\delta[y_{k,i} - 1] \end{aligned} \tag{4.4}$$

where $\Pr(y_{k,i} = 0|x_{k,i} = 0)$ is the probability that the sensed state of the ith channel is not occupied at time step k, given that the state of the ith channel is not occupied at time step k, and $\Pr(y_{k,i} = 1|x_{k,i} = 0)$, commonly referred to as the probability of false alarm (P_{FA}), is the probability that the sensed state of the ith channel is occupied at time step k, given that the state of the ith channel is not occupied at time step k.

The discrete probability density function that defines the sensed state of the ith channel at time step k, given that the state of the ith channel is occupied at time step k is given by

$$\begin{aligned} \mathrm{p}(y_{k,i}|x_{k,i} = 1) =& \Pr(y_{k,i} = 0|x_{k,i} = 1)\delta[y_{k,i} - 0] + \\ & \Pr(y_{k,i} = 1|x_{k,i} = 1)\delta[y_{k,i} - 1] \end{aligned} \tag{4.5}$$

where $\Pr(y_{k,i} = 0|x_{k,i} = 1)$, commonly referred to as the probability of missed detection (P_{MD}), is the probability that the sensed state of the ith channel is not occupied at time step k, given that the state of the ith channel is occupied at time step k, and $\Pr(y_{k,i} = 1|x_{k,i} = 1)$, commonly referred to as the probability of detection (P_{D}), is the probability that the sensed state of the ith channel is occupied at time step k, given that the state of the ith channel is occupied at time step k.

The values of P_{FA} and P_{MD} are provided by the spectrum sensing operation and are based upon the level of signal-to-noise ratio (SNR) and upon the spectrum sensing technique used. In our simulations, both P_{FA} and P_{MD} remain fixed with respect to time as we assume that channel conditions do not change.

4.3 Channel State Estimation

Using the dynamic state space formulation provided by the state model in Equations (4.2) and (4.3) and the measurement model in Equations (4.4) and (4.5), our goal is to estimate the channel occupancy state. In order to achieve that, we explore the use of an optimal Bayesian filter that uses grid-based methods to obtain the posterior probability density function at time step k. We also consider the sub-optimal Bayesian particle filter (PF) that estimates the posterior probability density function at time step k using a set of particles and weights.

4.3.1 Grid-based Bayesian Approach

The grid-based methods used by the optimal Bayesian filter provide the optimal recursion of the posterior probability density function if the state space is discrete and consists of a finite number of states [17]. The posterior probability density function is denoted by $\text{p}(\mathbf{x}_k|\mathbf{y}_{1:k})$, where the state vector is given by $\mathbf{x}_k = [x_{k,1} \ \ldots \ x_{k,N}]^T$ and the measurement data $\mathbf{y}_{1:k}$ up to time k is given by the set of measurement vectors $\{\mathbf{y}_1, \mathbf{y}_2, \ldots, \mathbf{y}_N\}$ and $\mathbf{y}_k = [y_{k,1} \ \ldots \ y_{k,N}]^T$ where T denotes the vector transpose. In our case, the state space at time k consists of 2^N discrete state vectors $\{\mathbf{x}_k^{[1]}, \mathbf{x}_k^{[2]}, \ldots, \mathbf{x}_k^{[2^N]}\}$ representing all possible combinations of channel occupancy.

The calculation of $\text{p}(\mathbf{x}_k|\mathbf{y}_{1:k})$, as discussed in [17], is a 2-step process consisting of

a prediction step,

$$\mathrm{p}(\mathbf{x}_k|\mathbf{y}_{1:k-1}) = \sum_{j=1}^{2^N} \mathrm{p}(\mathbf{x}_k|\mathbf{x}_{k-1}^{[j]})\mathrm{p}(\mathbf{x}_{k-1}^{[j]}|\mathbf{y}_{1:k-1}) \tag{4.6}$$

and an update step,

$$\mathrm{p}(\mathbf{x}_k|\mathbf{y}_{1:k}) = \frac{\mathrm{p}(\mathbf{y}_k|\mathbf{x}_k)\mathrm{p}(\mathbf{x}_k|\mathbf{y}_{1:k-1})}{\sum_{j=1}^{2^N} \mathrm{p}(\mathbf{y}_k|\mathbf{x}_k^{[j]})\mathrm{p}(\mathbf{x}_k^{[j]}|\mathbf{y}_{1:k-1})}. \tag{4.7}$$

Equations (4.6) and (4.7) result in the most accurate approach to obtain the channel state estimate. However, it is computationally very demanding, and infeasible for large values of N. For this reason, we do not explore its performance in our simulations, but we consider the sub-optimal PF instead.

4.3.2 Particle Filter Approach

The particle filter approximates the posterior probability density function with a set of particles and weights. The particles and weights can then be used to estimate the state [17]. The set of particles is denoted by $\{\mathbf{x}_k^{(1)}, \mathbf{x}_k^{(2)}, \ldots, \mathbf{x}_k^{(M)}\}$ where M is the number of particles and each particle is an $N \times 1$ vector $\mathbf{x}_k^m = [x_{k,1}^{(m)} \ \ldots \ x_{k,N}^{(m)}]^T$ where $x_{k,i}^{(m)}$ is the state of the ith channel occupancy at time step k for the mth particle. The corresponding set of weights is denoted by $\{w_k^{(1)}, w_k^{(2)}, \ldots, w_k^{(M)}\}$.

We use the sequential importance resampling (SIR) particle filter algorithm that is described in the following steps [17].

Step 1. For $m = 1, ..., M$ draw particle $\mathbf{x}_k^{(m)}$ from the importance sampling function $q(\mathbf{x}_k^{(m)}|\mathbf{x}_{k-1}^{(m)}, \mathbf{y}_k)$ and assign a weight, $w_k^{(m)}$, as shown in the following equation:

$$w_k^{(m)} \propto w_{k-1}^{(m)} \frac{\mathrm{p}(\mathbf{y}_k|\mathbf{x}_k^{(m)})\mathrm{p}(\mathbf{x}_k^{(m)}|\mathbf{x}_{k-1}^{(m)})}{q(\mathbf{x}_k^{(m)}|\mathbf{x}_{k-1}^{(m)}, \mathbf{y}_k)} \tag{4.8}$$

where $\mathbf{y}_k = [y_{k,1} \ \ldots \ y_{k,N}]^T$. We use the transition prior probability distribution, denoted by $\mathrm{p}(\mathbf{x}_k|\mathbf{x}_{k-1}^{(m)})$, which is obtained directly from our state transition model, as

the importance sampling function. This simplifies the calculation of the weights, as follows:

$$w_k^{(m)} \propto w_{k-1}^{(m)} \mathrm{p}(\mathbf{y}_k|\mathbf{x}_k^{(m)}) \tag{4.9}$$

where $\mathrm{p}(\mathbf{y}_k|\mathbf{x}_k^{(m)})$ is obtained from Equations (4.4) and (4.5).

Step 2. For $m = 1, \ldots, M$, we compute the normalized weights $w_k^{(m)}$ as follows:

$$w_k^{(m)} = \frac{w_k^{(m)}}{\sum_{m=1}^{M} w_k^{(m)}} \tag{4.10}$$

Step 3. We compute the number of effective samples, denoted by N_{eff}, as follows:

$$N_{\text{eff}} = \frac{1}{\sum_{m=1}^{M} \left(w_k^{(m)}\right)^2} \tag{4.11}$$

Step 4. If $N_{\text{eff}} < N_{\text{t}}$, where N_{t} is some predetermined threshold, then we perform resampling (with replacement) by drawing M particles from the current particle set $\{\mathbf{x}_k^1, \mathbf{x}_k^2, \ldots, \mathbf{x}_k^M\}$ with probabilities proportional to their weights. We replace the current particle set with the new set and calculate new weights using:

$$w_k^{(m)} = \frac{1}{M} \tag{4.12}$$

for all k.

The estimated posterior probability density function is thus given by:

$$\mathrm{p}(\mathbf{x}_k|\mathbf{y}_{1:k}) \approx \sum_{m=1}^{M} w_k^{(m)} \delta(\mathbf{x}_k - \mathbf{x}_k^{(m)}) \tag{4.13}$$

The set of particles and weights can then be used to obtain an estimate of the true state, denoted by $\hat{\mathbf{x}}_k$, as follows:

$$\hat{\mathbf{x}}_k = \mathrm{E}[\mathbf{x}_k] = \int \mathbf{x}_k(\mathbf{x}_k|\mathbf{y}_{1:k}) \mathrm{d}\mathbf{x}_k \approx \sum_{m=1}^{M} \left(w_k^{(m)} \mathbf{x}_k^{(m)}\right) \tag{4.14}$$

The result of Equation (4.14) is an $(N \times 1)$ vector in which each element takes on a value between 0 and 1. We therefore round our results towards the nearest integer in order to obtain our estimate of the discrete state.

In conclusion, the estimation result $\hat{\mathbf{x}}_k$ is a binary vector of the channel occupancy state. Specifically, if the ith element of $\hat{\mathbf{x}}_k$ is one, then the ith channel is estimated to be occupied; and if the ith element is zero, then the ith channel is estimated to not be occupied.

Chapter 5

SINGLE CHANNEL SELECTION

Multiple channels can be available to the secondary user for transmission at each time step, but, based on the assumption that a single channel provides adequate bandwidth for secondary user transmission, our goal is to find the channel with the minimum cost. This chapter discusses the use of a cost function to accomplish this goal. The cost function consists of a cost table listing the costs for each unique combination of input parameters. We assign low costs to desirable combinations of input parameters, and high costs to undesirable combinations. By minimizing the expected cost of the cost function over all possible channel selection hypotheses, we arrive at the optimal hypothesis which represents the optimal channel that will be used by the secondary user for transmission.

In Section 5.1, we discuss the cost table and explain how cost values are assigned based on the input parameters. In Section 5.2, we discuss the selection cost function, and present an example of how the cost table is used by the selection cost function. In Section 5.3, we show how the selection cost function, along with the particle filter state estimation in Section 4.3, is used to compute the expected cost associated with a single channel selection hypothesis.

5.1 Cost Table Formation

We use the cost table as a means to assign a single cost to each unique combination of input parameters. The three input parameters that we use are $x_{k,i}$, the ith channel occupancy at time step k, $H_k^{(\mathrm{ch})}$, the Channel ch selection hypothesis at time step k,

and $\hat{H}_{k-1}^{(\mathrm{ch})}$, the estimated Channel ch selection hypothesis at time step $k-1$. Each of these parameters is either assigned one of two possible values or it results in one of two possible outcomes. Overall, the three parameters yield eight combinations. The cost values within the cost table are assigned based on the the priority level of a given combination of input parameters. The higher the priority level of a parameter combination, the lower its assigned cost. The input parameters are described in Table 5.1.

Table 5.1: Description of parameters and their assigned or outcome values.

Parameter	Description	Assigned or Outcome Value
$H_k^{(\mathrm{ch})}$	Channel selection hypothesis at time step k taken from the hypotheses set $\{H_k^{(0)}, H_k^{(1)}, \ldots, H_k^{(N)}\}$	ch $= i$ or ch $\neq i$
$x_{k,i}$	State of occupancy of the ith channel at time step k	0 or 1
$\widehat{H}_{k-1}^{(\mathrm{ch})}$	Estimated channel selection hypothesis at time step $k-1$	ch $= i$ or ch $\neq i$

Assigning a cost to a given combination of parameters $H_k^{(\mathrm{ch})}$ and $x_{k,i}$, is equivalent to assigning a priority level to the combination with the goal of minimizing the primary user interference occurrences and the secondary user missed opportunities. A given combination of $H_k^{(\mathrm{ch})}$ and $x_{k,i}$ has a high priority level for either the primary user or the secondary user, but not both. The cost assignment based on priority levels is provided in Table 5.2. The assigned costs are unbiased in that the number of low and high priority combination levels occur equally between the primary and secondary users. In particular, unbiased costs place equal emphasis on minimizing

primary user interference occurrences and secondary user missed opportunities.

Table 5.2: Cost assignment based on priority levels of combinations of parameters $H_k^{(\text{ch})}$ and $x_{k,i}$. Here, SU stands for secondary user and PU stands for primary user.

$H_k^{(\text{ch})}$	$x_{k,i}$	Description	Priority Level	Cost
ch $\neq i$	$x_{k,i} = 0$	SU does not select channel that is not occupied by PU	Low priority level for SU	5
ch $\neq i$	$x_{k,i} = 1$	SU does not select channel that is occupied by PU	High priority level for PU	2
ch $= i$	$x_{k,i} = 0$	SU selects channel that is not occupied by PU	High priority level for SU	2
ch $= i$	$x_{k,i} = 1$	SU selects channel that is occupied by PU	Low priority level for PU	5

Assigning a cost to a given combination of parameters $H_k^{(\text{ch})}$ and $\widehat{H}_{k-1}^{(\text{ch})}$, is equivalent to assigning a priority level to the combination with the goal of minimizing channel switchings. Note that the priority level is only from the perspective of the secondary user since the primary user is not affected when the secondary user switches channels. In Table 5.3, we describe each combination of $H_k^{(\text{ch})}$ and $\widehat{H}_{k-1}^{(\text{ch})}$, and assign costs based on the priority level of each combination. The costs associated with high priority level combinations are not as low as the ones for high priority level combinations in Table 5.2 because we consider minimizing primary user interference occurrences and secondary user missed opportunities to be more important than minimizing channel switchings; similarly, the costs associated with low priority level combinations are not as high as the ones for low priority level combinations in Table 5.2.

Finally, by combining Table 5.2 and Table 5.3, we form the cost lookup table

Table 5.3: Cost assignment based on priority levels of combinations of parameters $H_k^{(\mathrm{ch})}$ and $\widehat{H}_{k-1}^{(\mathrm{ch})}$. Here, SU stands for secondary user and PU stands for primary user.

$H_k^{(\mathrm{ch})}$	$\widehat{H}_{k-1}^{(\mathrm{ch})}$	Description	Priority Level	Cost
$\mathrm{ch} \neq i$	$\mathrm{ch} \neq i$	SU does not select channel that was not selected at previous time step	High priority level for SU	3
$\mathrm{ch} \neq i$	$\mathrm{ch} = i$	SU does not select channel that was selected at previous time step	Low priority level for SU	4
$\mathrm{ch} = i$	$\mathrm{ch} \neq i$	SU selects channel that was not selected at previous time step	Low priority level for SU	4
$\mathrm{ch} = i$	$\mathrm{ch} = i$	SU selects channel that was selected at previous time step	High priority level for SU	3

shown in Table 5.4, which is used by the selection cost function (SCF) in the next section.

Table 5.4: Cost assignment for parameters $H_k^{(\text{ch})}$, $\widehat{H}_{k-1}^{(\text{ch})}$, and $x_{k,i}$.

$H_k^{(\text{ch})}$	$\widehat{H}_{k-1}^{(\text{ch})}$	$x_{k,i}$	$g(H_k^{(\text{ch})}, \hat{H}_{k-1}^{(\text{ch})}, x_{k,i})$
ch $\neq i$	ch $\neq i$	0	8
ch $\neq i$	ch $\neq i$	1	5
ch $\neq i$	ch $= i$	0	9
ch $\neq i$	ch $= i$	1	6
ch $= i$	ch $\neq i$	0	6
ch $= i$	ch $\neq i$	1	9
ch $= i$	ch $= i$	0	5
ch $= i$	ch $= i$	1	8

5.2 Heuristic Selection Cost Function

The SCF is used to calculate the total cost for a given $H_k^{(\text{ch})}$, $\widehat{H}_{k-1}^{(\text{ch})}$, and $\mathbf{x}_k = [x_{k,1} \ \ldots \ xk, N]^T$ as follows:

$$G\left(H_k^{(\text{ch})}, \widehat{H}_{k-1}^{(\text{ch})}, \mathbf{x}_k\right) = \sum_{i=1}^{N} g\left(H_k^{(\text{ch})}, \widehat{H}_{k-1}^{(\text{ch})}, x_{k,i}\right) \tag{5.1}$$

where the cost function $g(\cdot)$ for the different values of $H_k^{(\text{ch})}$, $\hat{H}_{k-1}^{(\text{ch})}$, and $x_{k,i}$) is obtained from Table 5.4. The table lookup arguments $H_k^{(\text{ch})}$, $\widehat{H}_{k-1}^{(\text{ch})}$, and $x_{k,i}$ serve as the indices into the table, and the matching cost value is returned. The cost lookup table provides a single cost for every possible unique combination of $H_k^{(\text{ch})}$, $\widehat{H}_{k-1}^{(\text{ch})}$, and $x_{k,i}$.

An example of cost lookup using the SCF is given as follows. Assume that the secondary user has sensed $N = 3$ channels. At time step k, channels 1 and 2 are unoccupied, and channel 3 is occupied; thus $\mathbf{x}_k = [001]^T$. Assume that at time

step $k-1$, channel 2 was selected for transmission; therefore, the estimated channel selection hypothesis at time step $k-1$ is denoted by $\widehat{H}_k^{(2)}$. We want to calculate the cost associated with each channel selection hypothesis at time step k from the set $\{H_k^{(0)}, H_k^{(1)}, H_k^{(2)}, H_k^{(3)}\}$ in order to choose the channel for transmission by the secondary user with the minimum cost.

Starting with the null hypothesis in which no channel is selected, denoted by $H_k^{(0)}$, we insert $H_k^{(0)}$, $\widehat{H}_k^{(2)}$, and $\mathbf{x}_k = [001]$ into Equation (5.1), and proceed to calculate the cost for each channel as follows.

For $i = 1$, the arguments to the cost table are $H_k^{(0)}$ (where ch $\neq i$), $\widehat{H}_k^{(2)}$ (where ch $\neq i$), and $x_{k,i} = 0$. The cost associated with this unique combination of arguments is $g(0, 2, 0) = 8$, (first row of Table 5.4).

For $i = 2$, the arguments to the cost table are $H_k^{(0)}$ (where ch $\neq i$), $\widehat{H}_k^{(2)}$ (where ch $= i$), and $x_{k,i} = 0$. The cost associated with this unique combination of arguments is $g(0, 2, 0) = 9$, (third row of Table 5.4).

For $i = 3$, the arguments to the cost table are $H_k^{(0)}$ (where ch $\neq i$), $\widehat{H}_k^{(2)}$ (where ch $\neq i$), and $x_{k,i} = 1$. The cost associated with this unique combination of arguments is $g(0, 2, 1) = 5$, (second row of Table 5.4).

The total cost associated with $H_k^{(0)}$, as obtained from Equation (5.1), is thus $G(H_k^{(\text{ch})}, \widehat{H}_{k-1}^{(\text{ch})}, \mathbf{x}_k) = g(0, 2, 0) + g(0, 2, 0) + g(0, 2, 1) = 22$. Similarly, the total cost associated with $H_k^{(1)}$ is $6+9+5 = 20$, the total cost associated with $H_k^{(2)}$ is $8+5+5 = 18$, and the total cost associated with $H_k^{(3)}$ is $8 + 9 + 9 = 26$. The costs obtained imply that channel 2 is the most desirable channel because it is currently unoccupied and it was selected at the previous time step.

5.3 Theoretic Selection Cost Function

5.3.1 Computation of Expected Cost using Particle Filter

In order to obtain the expected cost associated with a given channel selection hypothesis $H_k^{(\mathrm{ch})}$, we consider the state of channel occupancy to be a random variable with a corresponding posterior probability density function $\mathrm{p}(\mathbf{x}_k|\mathbf{y}_{1:k})$ that we estimated using the PF in Chapter 4. The expected cost function can be obtained as

$$\mathrm{E}\left[G(H_k^{(\mathrm{ch})}, \widehat{H}_{k-1}^{(\mathrm{ch})}, \mathbf{x}_k)\right] = \int G(H_k^{(\mathrm{ch})}, \widehat{H}_{k-1}^{(\mathrm{ch})}, \mathbf{x}_k)\mathrm{p}(\mathbf{x}_k|\mathbf{y}_{1:k})\mathrm{d}\mathbf{x}_k \tag{5.2}$$

where the posterior distribution is approximated using the PF as

$$\mathrm{E}\left[G(H_k^{(\mathrm{ch})}, \widehat{H}_{k-1}^{(\mathrm{ch})}, \mathbf{x}_k)\right] = \sum_{m=1}^{M} G(H_k^{(\mathrm{ch})}, \widehat{H}_{k-1}^{(\mathrm{ch})}, \mathbf{x}_k^{(m)})w_k^{(m)} \tag{5.3}$$

We refer to Equation (5.3) as the direct PF (DPF) method because the particles and weights are used directly in the expected cost function.

We can also use the state estimated by the PF in the expected cost function, which simplifies the calculation to the following:

$$\mathrm{E}\left[G(H_k^{(\mathrm{ch})}, \widehat{H}_{k-1}^{(\mathrm{ch})}, \mathbf{x}_k)\right] = G(H_k^{(\mathrm{ch})}, \widehat{H}_{k-1}^{(\mathrm{ch})}, \hat{\mathbf{x}}_k) \tag{5.4}$$

We refer to Equation (5.4) as the indirect PF (IPF) method because the particles and weights are used indirectly to produce the estimated state $\hat{\mathbf{x}}_k$, which is then used in the expected cost function.

If the secondary user is operating in a very high signal-to-noise ratio (SNR) environment, we can assume that the sensed state is a perfect measurement of the true state. In this case, the expected cost is calculated as follows:

$$\mathrm{E}\left[G(H_k^{(\mathrm{ch})}, \widehat{H}_{k-1}^{(\mathrm{ch})}, \mathbf{x}_k)\right] = G(H_k^{(\mathrm{ch})}, \widehat{H}_{k-1}^{(\mathrm{ch})}, \mathbf{y}_k) \tag{5.5}$$

We refer to Equation (5.5) as the direct sensing (DS) method because the the sensed state of channel occupancy $\mathbf{y}_k$ is used directly in the expected cost function.

5.3.2 Minimum Selection Cost Function

The optimal channel selection hypothesis at time step k, denoted by $\widehat{H}_k^{(\mathrm{ch})}$, is made by minimizing the expected cost over all possible channel selection hypotheses. This is shown as follows:

$$\widehat{H}_k^{(\mathrm{ch})} = \underset{H_k^{(0)}, H_k^{(1)}, \ldots, H_k^{(M)}}{\arg\min} \mathrm{E}\left[G(H_k^{(\mathrm{ch})}, \widehat{H}_{k-1}^{(\mathrm{ch})}, \mathbf{x}_k) \right] \tag{5.6}$$

Chapter 6

SIMULATIONS

In this chapter, we explore the performance of the particle filter, and compare the various channel selection techniques. We simulate a variety of environments ranging from a low to high number of primary user channels, low to high levels of signal-to-noise ratio, and low to high levels of primary user traffic.

In Section 6.1, we discuss the values assigned to the various simulation parameters. In Section 6.2, we explore the performance of the particle filter and determine the number of particles necessary to achieve a desired level of performance. In Section 6.3, we compare the performance of the various channel selection techniques.

6.1 Simulation Parameters

Throughout our simulations, we use 3 different values of N, corresponding to low, medium, and high levels of channel density. The specific values we assign to N for each of 3 channel density levels is shown in Table 6.1.

Table 6.1: Simulation values associated with various channel density levels.

Channel density	N
Low	6
Medium	12
High	18

Regarding our measurement model parameters, we use 3 different probability of

false alarm (P_{FA}) and probability of detection (P_{D}) value pairs. These 3 value pairs correspond to low, medium, and high levels of sensing accuracy. The specific values we assign to P_{FA} and P_{D} for each of the 3 sensing accuracy levels are shown in Table 6.2. These are values that would appear on a typical receiver operating characteristic curve, as seen in [6], where the low values correspond to a low-performance spectrum sensing algorithm and/or low levels of signal-to-noise ratio (SNR), the medium values correspond to a medium-performance spectrum sensing algorithm and/or medium levels of SNR, and the high values correspond to a high-performance spectrum sensing algorithm operating in high levels of SNR.

Table 6.2: Simulation values associated with various sensing accuracy levels.

Sensing accuracy	P_{FA}	P_{D}
Low	.4	.5
Medium	.1	.85
High	.01	.95

Regarding our state model parameters, similar to [14], we use three levels of primary user traffic, namely low, medium and high. Low traffic has the characteristics of long unoccupied durations and short occupied durations, while high traffic is characterized by long occupied durations and short unoccupied durations. Medium traffic falls in between. Simulations are also performed for a mixed traffic scenario in which a third of the channels have low traffic, a third have medium traffic, and a third have high traffic. The specific values we assign to the state model parameters for each of the 3 traffic levels are shown in Table 6.3. The state model parameters that correspond to probabilities of occupancy for the ith channel are $\Pr(x_{0,i} = 1)$, $\Pr(x_{k,i} = 1|x_{k-1,i} = 0)$, and $\Pr(x_{k,i} = 1|x_{k-1,i} = 1)$. The state model parameters that correspond to probabilities of unoccupancy for the ith channel are $\Pr(x_{0,i} = 0)$,

$\Pr(x_{k,i} = 0|x_{k-1,i} = 0)$, and $\Pr(x_{k,i} = 0|x_{k-1,i} = 1)$.

Table 6.3: Simulation values associated with various traffic levels.

Traffic	Probability of channel occupancy $\Pr(x_{0,i} = 1)$ $\Pr(x_{k,i} = 1\|x_{k-1,i} = 0)$ $\Pr(x_{k,i} = 1\|x_{k-1,i} = 1)$	Probability of channel unoccupancy $\Pr(x_{0,i} = 0)$ $\Pr(x_{k,i} = 0\|x_{k-1,i} = 0)$ $\Pr(x_{k,i} = 0\|x_{k-1,i} = 1)$
Low	0.1	0.9
Medium	0.5	0.5
High	0.9	0.1

6.2 Particle Filter Simulations

Before using the particle filter (PF) in the channel selection simulations, we must determine an appropriate number of particles, denoted by M, to use for various combinations of simulation parameters to obtain accurate channel occupancy estimates. There exists a trade off between high accuracy of the particle filter and processing time required to obtain that high level of accuracy. We measure the accuracy of the PF in terms of mean square error (MSE). The calculation of PF MSE at time step k, denoted by MSE_k, is shown below:

$$\text{MSE}_k = \frac{1}{N}\sum_{i=1}^{N}\left(x_{k,i} - \sum_{m=1}^{M}\left(w_k^{(m)}x_{k,i}^{(m)}\right)\right)^2 \tag{6.1}$$

The calculation of the overall MSE across all K time steps is shown below:

$$\text{MSE} = \frac{1}{K}\sum_{k=1}^{K}\text{MSE}_k \tag{6.2}$$

In a similar manner, we can calculate the MSE of the sensed state of channel occupancy provided by the spectrum sensing (SS) operation by substituting $y_{k,i}$ for

$\sum_{m=1}^{M} \left(w_k^{(m)} x_{k,i}^{(m)} \right)$ in Equation (6.1). We refer to this as the SS MSE, and it provides us with a benchmark against which to compare the PF MSE.

We run multiple simulations which correspond to each possible combination of channel density, sensing accuracy, and traffic taken from Table 6.1, Table 6.2, and Table 6.3. Each simulation is made up of multiple simulation runs in which we vary the value of M from 2^0 to 2^{10}. In each simulation run, we set the number of time steps K to 100, and average both the PF MSE, and the SS MSE results over 10 simulation iterations.

Some of these results corresponding to low, medium and high sensing accuracy are shown in Figure 6.1. In each of the plots, the channel density is fixed to medium and the traffic is mixed, i.e., a third of the channels have low traffic, a third have medium traffic, and a third have high traffic.

By examining all PF simulation results, we determine the number of particles to use for a given level of sensing accuracy, channel density, and traffic. This information, along with the PF MSE associated with the specified number of particles, and the SS MSE, is summarized in Table 6.4, Table 6.5, and Table 6.6. The last column in the tables is the result of subtracting the PF MSE from the SS MSE. If the value in this column is positive, then the PF estimated state is more accurate than the sensed state. If the value is negative, then the sensed state is more accurate than the PF estimated state.

What we have found is that the levels of sensing accuracy and traffic have the greatest impact on PF MSE, and therefore dictate the number of particles required to obtain accurate results in terms of PF MSE as compared to SS MSE. For medium traffic level, a much larger number of particles is required than for low or high traffic level. Each increase in sensing accuracy from low to medium to high requires an increased number of particles, regardless of the levels of traffic and channel density.

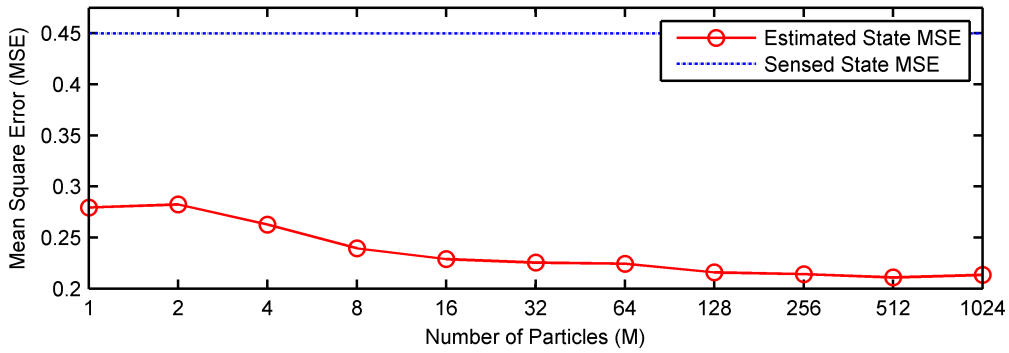

(a) Low sensing accuracy

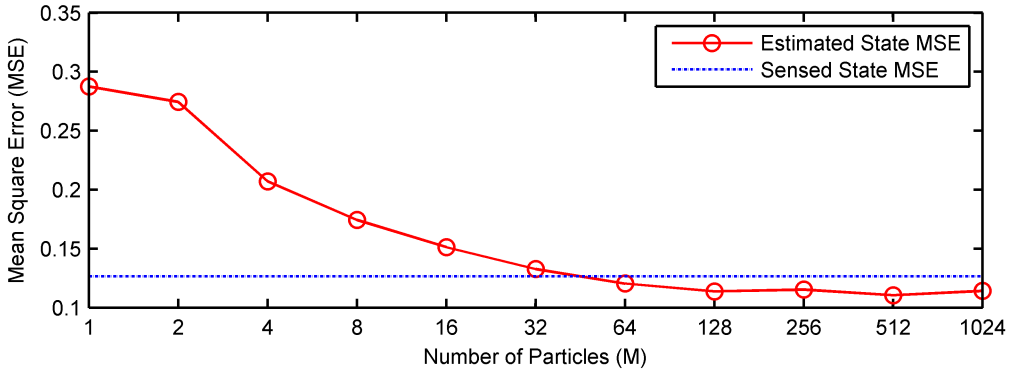

(b) Medium sensing accuracy

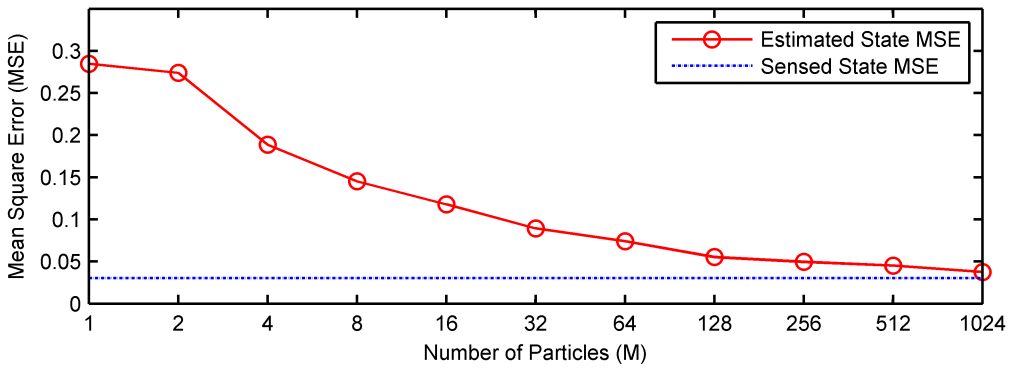

(c) High sensing accuracy

Figure 6.1: Particle filter MSE plotted versus the number of particles M, with medium channel density and mixed traffic.

Table 6.4: Low sensing accuracy particle filter simulation results.

Channel Density	Traffic	Particles	PF MSE	SS MSE	SS MSE - PF MSE
Low	Low	16	0.1090	0.4082	0.2992
Low	Medium	256	0.4493	0.4499	0.0006
Low	High	16	0.0990	0.4938	0.3948
Low	Mixed	16	0.2290	0.4500	0.2210
Medium	Low	16	0.0972	0.4083	0.3111
Medium	Medium	512	0.4493	0.4486	-0.0007
Medium	High	16	0.1021	0.4911	0.3890
Medium	Mixed	16	0.2288	0.4497	0.2209
High	Low	16	0.1008	0.4117	0.3109
High	Medium	512	0.4518	0.4513	-0.0005
High	High	16	0.1013	0.4891	0.3878
High	Mixed	16	0.2310	0.4507	0.2197

Because channel density does not appear to have much of an impact on PF MSE, we fix the channel density level to medium for the channel selection simulation in the following section.

Table 6.5: Medium sensing accuracy particle filter simulation results.

Channel Density	Traffic	Particles	PF MSE	SS MSE	SS MSE - PF MSE
Low	Low	32	0.0952	0.1052	0.0100
Low	Medium	64	0.1317	0.1262	-0.0055
Low	High	32	0.1137	0.1446	0.0309
Low	Mixed	32	0.1108	0.1235	0.0127
Medium	Low	32	0.0998	0.1042	0.0044
Medium	Medium	512	0.1324	0.1235	-0.0089
Medium	High	32	0.1172	0.1465	0.0293
Medium	Mixed	128	0.1138	0.1266	0.0128
High	Low	32	0.0980	0.1037	0.0057
High	Medium	512	0.1863	0.1252	-0.0611
High	High	32	0.1122	0.1459	0.0337
High	Mixed	256	0.1124	0.1258	0.0134

Table 6.6: High sensing accuracy particle filter simulation results.

Channel Density	Traffic	Particles	PF MSE	SS MSE	SS MSE - PF MSE
Low	High	256	0.0525	0.0468	-0.0057
Low	Mixed	256	0.0348	0.0309	-0.0039
Medium	Low	256	0.0239	0.0142	-0.0097
Medium	Medium	1024	0.0560	0.0300	-0.0260
Medium	High	256	0.0681	0.0470	-0.0211
Medium	Mixed	1024	0.0376	0.0301	-0.0075
High	Low	256	0.0369	0.0136	-0.0233
High	Medium	1024	0.1244	0.0298	-0.0946
High	High	256	0.0697	0.0461	-0.0236
High	Mixed	1024	0.0531	0.0300	-0.0231

6.3 Channel Selection Simulations

Following a similar approach as the simulations in [8] and [9], we use a random selection technique as a baseline against which to compare our cost-based channel selection techniques. In the random selection technique, we use the sensed state information $\mathbf{y}_k$. An unoccupied channel is selected randomly and is used until the channel becomes occupied. In our plots, we refer to the random selection technique as RND. The RND technique, along with the other channel selection techniques discussed in Section 5.3 are summarized in Table 6.7.

Table 6.7: Summary of channel selection simulation techniques.

Technique	Description
Random (RND)	Use the sensed state $\mathbf{y}_k$.
Direct sensing (DS)	Use the sensed state $\mathbf{y}_k$ directly in the SCF.
Indirect particle filter (IPF)	Use particles and weights indirectly to produce the estimated state $\mathbf{x}_k$, which is then used in the SCF.
Direct particle filter (DPF)	Use particles and weights directly in the SCF.

Based on the low priority level scenarios discussed in Section 5.1, we formulate a set of simulation metrics which we use to compare the performance of the various channel selection techniques. These metrics are summarized in Table 6.8.

In each of the channel selection simulations, we set the number of time steps K to 100, and we calculate the metrics in Table 5.1 as a percentage of K, averaged over 10 simulation iterations. We fix the level of channel density to medium, for all channel selection simulations.

Table 6.8: Summary of channel selection simulation metrics. Here, SU stands for secondary user and PU stands for primary user.

Metric	Description	Formulation
PU interference	SU selects channel that is occupied by PU	$\widehat{H}_k^{(i)}, x_{k,i} = 1$
SU missed opportunity	SU does not select any channel when at least one channel is available	$\widehat{H}_k^{(0)}, \sum x_{k,i} \neq N$
Channel switch	SU selects channel that was not selected at previous time step	$\widehat{H}_k \neq \widehat{H}_{k-1}$

First we explore the performance of the various channel selection techniques in a low sensing accuracy environment. The number of particles used in the PF for each simulation is obtained from Table 6.4. The results, as shown in Figure 6.2, indicate that the IPF and DPF techniques consistently result in a significantly lower number of channel switches compared to the RND and DS techniques, regardless of the traffic level. In mixed traffic, the IPF and DPF techniques also result in a lower number of both primary user interference occurrences and secondary user missed opportunities when compared to the RND and DS techniques.

Next we explore the performance of the various channel selection techniques in a medium sensing accuracy environment. The number of particles used in the PF for each simulation is obtained from Table 6.5. The results, as shown in Figure 6.3, indicate that IPF and DPF techniques consistently result in a lower number of channel switches compared to the RND and DS techniques, regardless of the traffic level. However, the IPF and DPF techniques to not appear to offer any benefit over the

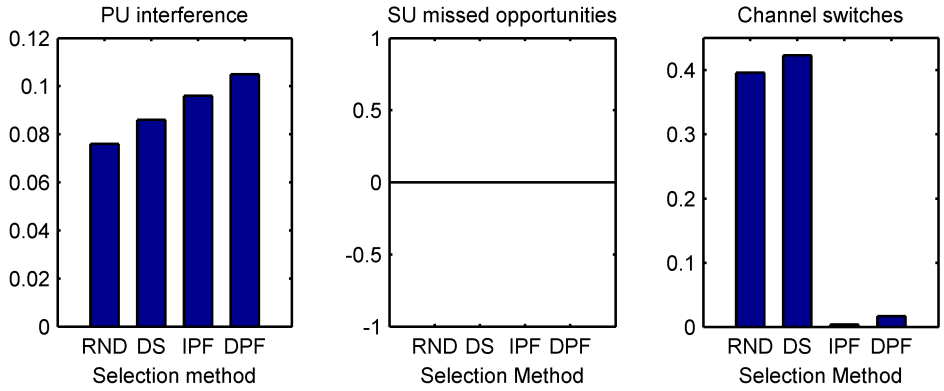

(a) Low traffic

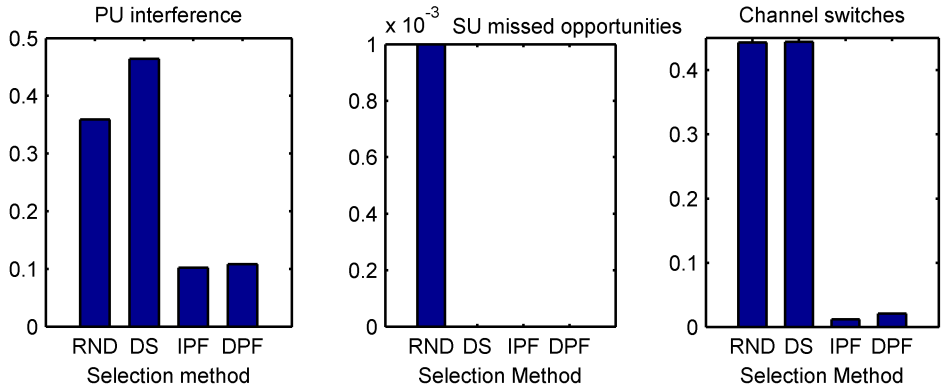

(b) Mixed traffic

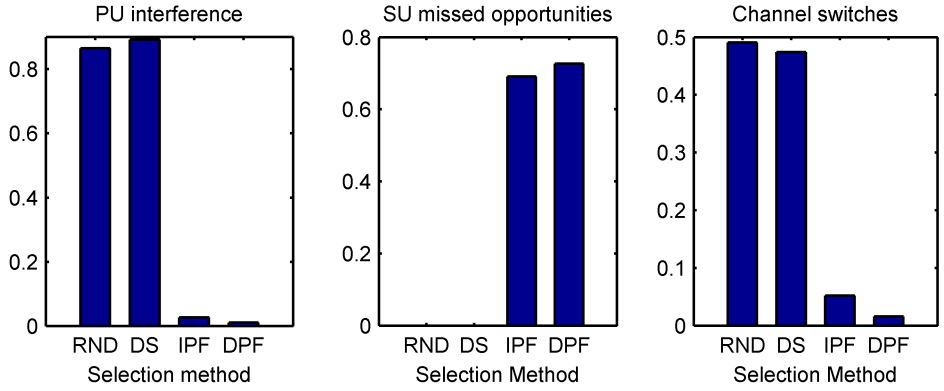

(c) High traffic

Figure 6.2: Channel selection technique performance, with low sensing accuracy.

RND and DS techniques in terms of both primary user interference and secondary user missed opportunities, regardless of the traffic level.

Finally we explore the performance of the various channel selection techniques in a high sensing accuracy environment. The number of particles used in the PF for each simulation is obtained from Table 6.6. The results, as shown in Figure 6.4, indicate that the IPF and DPF techniques offer a slight advantage over the RND and DS techniques in terms of channel switches, regardless of the traffic level. However, the IPF and DPF techniques to not appear to offer any benefit over the RND and DS techniques in terms of both primary user interference and secondary user missed opportunities, regardless of the traffic level.

In conclusion, we can see from the channel selection simulation results that the random and direct sensing techniques provide similar results, regardless of sensing accuracy and traffic levels. When the random technique is compared to the direct and indirect PF techniques, on the other hand, we can see that there is a clear advantage to using either the direct or indirect PF technique under certain conditions. Specifically when sensing accuracy is low and traffic is mixed, we can see that the use of either the direct or indirect PF technique results in a decrease in primary user interference by a factor of 3, and a decrease in channel switches by a factor of 20. There does not appear to be an advantage to using the direct PF technique over the indirect PF technique.

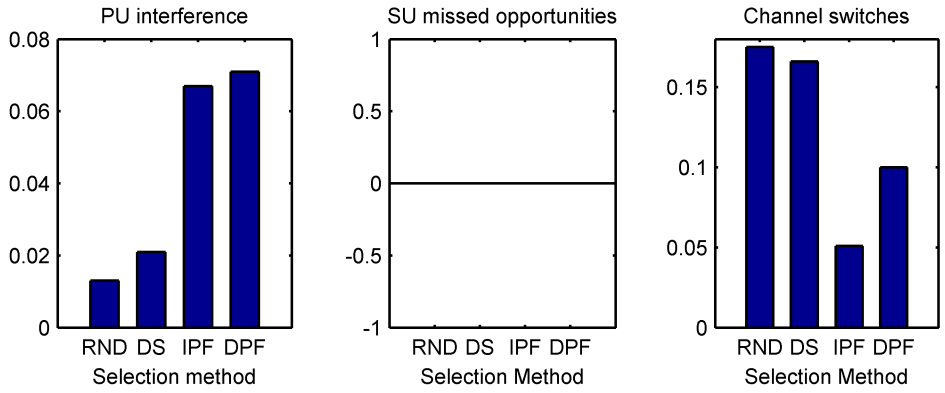

(a) Low traffic

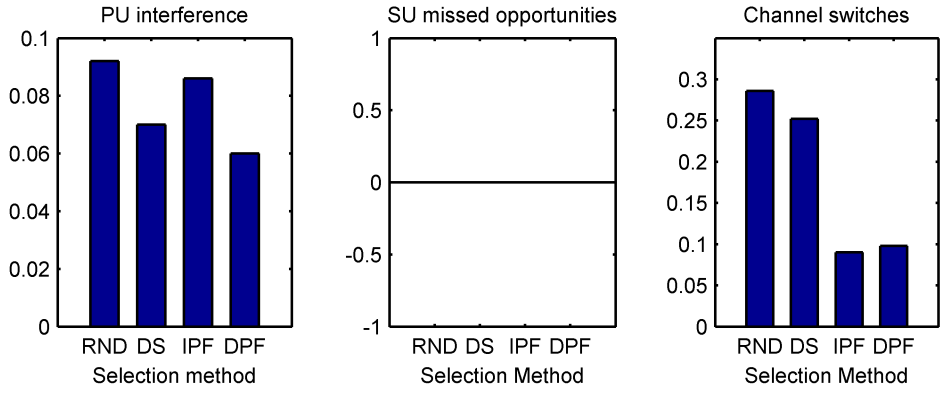

(b) Mixed traffic

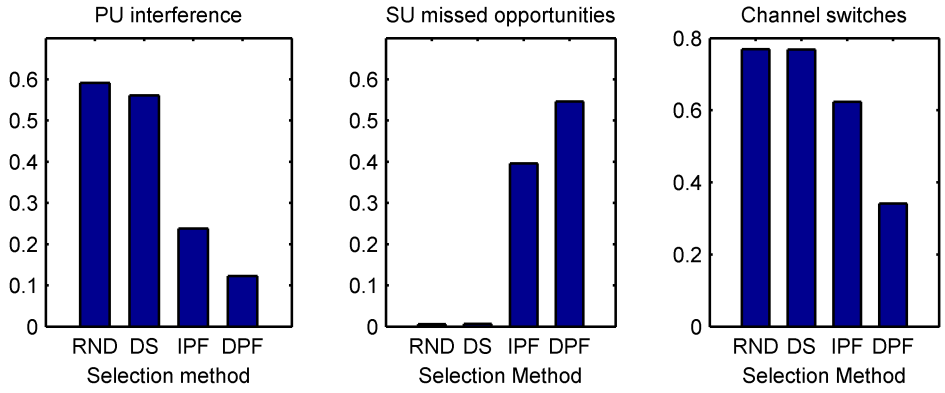

(c) High traffic

Figure 6.3: Channel selection technique performance, with medium sensing accuracy.

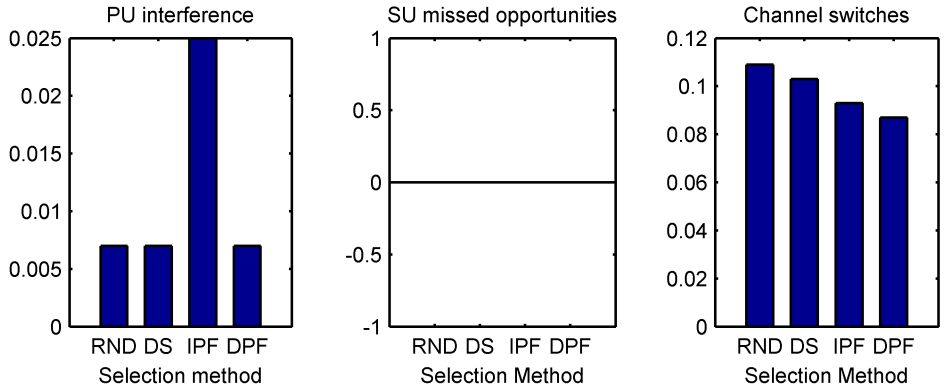

(a) Low traffic

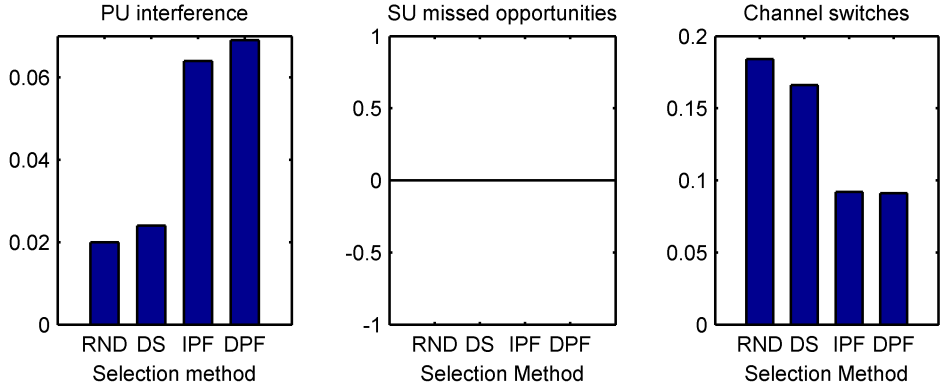

(b) Mixed traffic

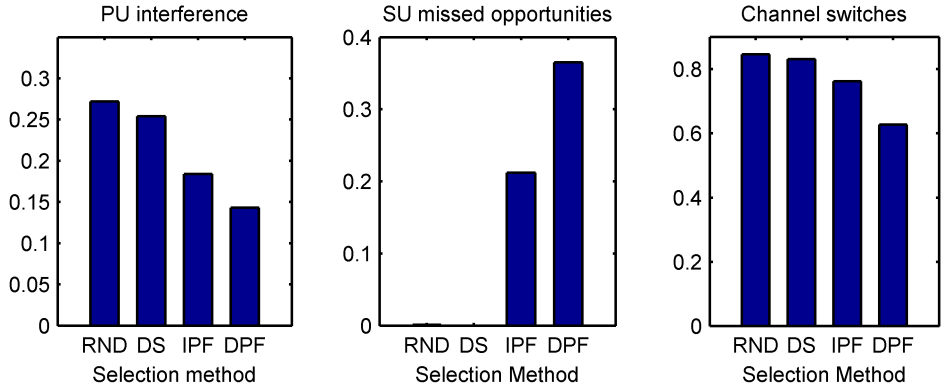

(c) High traffic

Figure 6.4: Channel selection technique performance with high sensing accuracy.

Chapter 7

CONCLUSIONS AND FUTURE WORK

We proposed a unique formulation of channel selection in cognitive radio as a dynamic state space estimation problem. We then estimated the channel occupancy using the particle filter sequential Monte Carlo method. By incorporating the particle filter into a selection cost function, we designed a method to select a single channel for secondary user transmission with the minimum cost function for channel occupancy at each time step. Using simulations, we demonstrated that the proposed method effectively decreases primary user interference, secondary user missed opportunities, and channel switches under certain conditions, when compared to a random channel selection technique.

When using the sensed state in the direct sensing technique, we did not find any advantage in applying the selection cost function over the random channel selection technique, irrespective of the level of sensing accuracy. On the other hand, when using the estimated state in both the direct and indirect particle filter techniques, we found a distinct advantage in applying the selection cost function over the random channel selection technique, under certain conditions. Specifically, when sensing accuracy is low and traffic is mixed, we have shown that primary user interference can be decreased by a factor of 3, and channel switches can be decreased by a factor of 20. We have also shown that the indirect particle filter technique performs nearly as well as the computationally intensive direct particle filter technique.

Regarding future work, the selection cost function is an area of research with many open questions to explore, especially with regards to input parameters. For example, channel switches could be further minimized by including a future channel occupancy

parameter. Throughput could be considered by including a channel bandwidth parameter. Furthermore, by pre-defining multiple costs for each combination of input parameters, the costs could be changed in real-time, thus allowing for a priority or objective-based channel selection scheme.

We would also like to extend our network model from a single secondary user to multiple secondary users, and look more closely at the interaction between secondary user source-destination pairs. We would like to expand our channel occupancy state model to a more realistic time-varying model. And finally, we would like to explore the hardware implementation of the particle filter and selection cost function in order to study real-time performance and determine practical feasibility.

REFERENCES

[1] A. M. Wyglinski, M. Nekovee, and T. Hou, Eds., *Cognitive Radio Communications and Networks: Principles and Practice*. Academic Press/Elsevier, 2009.

[2] S. Haykin, D. J. Thomson, and J. H. Reed, "Spectrum sensing for cognitive radio," *Proceedings of the IEEE*, vol. 97, no. 5, pp. 849–877, May 2009.

[3] T. Ikuma and M. Naraghi-Pour, "A comparison of three classes of spectrum sensing techniques," in *IEEE Global Telecommunications Conference*, New Orleans, LO, December 2008, pp. 1–5.

[4] S. Ziafat, W. Ejaz, and H. Jamal, "Spectrum sensing techniques for cognitive radio networks: Performance analysis," in *IEEE MTT-S International Microwave Workshop Series on Intelligent Radio for Future Personal Terminals*, Daejeon, August 2011, pp. 1–4.

[5] M. A. Abdulsattar and Z. A. Hussein, "Energy detection techniques for spectrum sensing in cognitive radio: A survey," *International Journal of Computer Networks & Communications*, vol. 4, no. 5, pp. 223–242, October 2012.

[6] S. Hossain, I. Abdullah, and M. A. Hossain, "Energy detection performance of spectrum sensing in cognitive radio," *International Journal of Information Technology & Computer Science*, vol. 4, no. 11, pp. 11–17, October 2012.

[7] T. Yucek and H. Arslan, "A survey of spectrum sensing algorithms for cognitive radio applications," *IEEE Communications Surveys & Tutorials*, vol. 11, no. 1, pp. 116–130, March 2009.

[8] V. Mishra, L. C. Tong, and C. Syin, "Deterministic time pattern based channel selection in cognitive radio network," in *International Conference on Information Networking*, Bangkok, January 2013, pp. 169–174.

[9] M. Bennai, J. Sydor, and M. Rahman, "Automatic channel selection for cognitive radio systems," in *IEEE 21st International Symposium on Personal Indoor and Mobile Radio Communications*, September 2010, pp. 1831–1835.

[10] L.-H. Kung, "Channel selection for cognitive radio terminals," Stanford University, Tech. Rep. CS229 Project Report, December 2008.

[11] Y. Song, Y. Fang, and Y. Zhang, "Stochastic channel selection in cognitive radio networks," in *Global Telecommunications Conference*, Washington, DC, November 2007, pp. 4878–4882.

[12] F. Hou and J. Huang, "Dynamic channel selection in cognitive radio network with channel heterogeneity," in *IEEE Global Telecommunications Conference*, Miami, FL, December 2010, pp. 1–6.

[13] D. Xu, E. Jung, and X. Liu, "Optimal bandwidth selection in multi-channel cognitive radio networks: How much is too much?" in *3rd IEEE Symposium on New Frontiers in Dynamic Spectrum Access Networks*, Chicago, IL, October 2008, pp. 1–11.

[14] P. N. Anggraeni, N. H. Mahmood, J. Berthod, N. Chaussonniere, L. My, and H. Yomo, "Dynamic channel selection for cognitive radios with heterogenous primary bands," *Wireless Personal Communications*, vol. 45, no. 3, pp. 369–384, May 2008.

[15] K. Liu, Q. Zhao, and B. Krishnamachari, "Dynamic multichannel access with imperfect channel state detection," *IEEE Transactions on Signal Processing*, vol. 58, no. 5, pp. 2795–2808, May 2010.

[16] A. Kaushik, M. Mueller, and F. K. Jondral, "Cognitive relay: Detecting spectrum holes in a dynamic scenario," in *Proceedings of the Tenth International Symposium on Wireless Communication Systems*, Ilmenau, Germany, August 2013, pp. 1–2.

[17] M. S. Arulampalam, S. Maskell, N. Gordon, and T. Clapp, "A tutorial on particle filters for online nonlinear/non-Gaussian Bayesian tracking," *IEEE Transactions on Signal Processing*, vol. 50, no. 2, pp. 174–188, February 2002.

[18] J. Mitola and G. Q. Maguire, "Cognitive radio: Making software radios more personal," *IEEE Personal Communications*, vol. 6, no. 4, pp. 13–18, August 1999.

[19] S. Haykin, "Cognitive radio: Brain-empowered wireless communications," *IEEE Journal on Selected Areas in Communication*, vol. 23, no. 2, pp. 201–220, February 2005.

[20] J. Mitola, "Software radios: Survey, critical evaluation and future directions," in *National Telesystems Conference*, vol. 13, Washington, DC, May 1992, pp. 15–23.

[21] NTIA. (2003, October) United states frequency allocations: The radio spectrum. [Online]. Available: www.ntia.doc.gov/osmhome/allochrt.PDF

[22] Siemens. (2010, January) 500 megabits/second with white led light. [Online]. Available: http://www.siemens.com/innovation/en/news/2010/500-megabits-second-with-white-led-light.htm

[23] M. A. McHenry, D. McCloskey, D. Roberson, and J. T. MacDonald, "Spectrum occupancy measurements: Chicago, Illinois: November 16-18, 2005," Shared Spectrum Company, Vienna, Virginia, Tech. Rep., December 2005.

[24] J. Mitola, "Cognitive radio: An integrated agent architecture for software defined radio," Ph.D. dissertation, Royal Institute of Technology, Stockholm, Sweden, 2000.

[25] "IEEE standard definitions and concepts for dynamic spectrum access: Terminology relating to emerging wireless networks, system functionality, and spectrum management," IEEE, New York, New York, Tech. Rep. 1900.1-2008, September 2008.

[26] K. Sithamparanathan and A. Giorgetti, *Cognitive Radio Techniques: Spectrum Sensing, Interference Mitigation, and Localization*. Norwood, MA: Artech House, 2012.

[27] H. Arslan, Ed., *Cognitive Radio, Software Defined Radio, and Adaptive Wireless Systems*. Springer Netherlands, 2007.

[28] B. A. Fette, Ed., *Cognitive Radio Technology*, 2nd ed. Burlington, MA: Academic Press/Elsevier, 2009.

[29] E. N. Gilbert, "Capacity of a burst-noise channel," *Bell System Technical Journal*, vol. 39, no. 5, pp. 1253–1265, September 1960.